# Mössbauer Study of $^{57}$Fe-doped Simple and Mixed Dihydrated Oxalates of Bivalent Metals (M = Mg, Mn, Fe, Co, Ni, Zn)

M. DEVILLERS, J. LADRIÈRE and D. APERS

*Université Catholique de Louvain, Laboratoire de Chimie Inorganique et Nucléaire, Chemin du Cyclotron 2, B-1348 Louvain-la-Neuve, Belgium*

(Received July 30, 1986)

## Abstract

Mössbauer spectroscopy is used to characterize the physico-chemical environment of $^{57}$Fe in isomorphous dihydrated oxalates of some bivalent metals (M = Mg, Mn, Fe, Co, Ni and Zn). Local covalency and lattice effects of the host matrix have been evidenced from accurate measurements of $^{57}$Fe quadrupole splitting. Such effects have also been observed in mixed Fe(II)/Co(II) and Fe(II)/Ni(II) oxalates over the whole concentration range.

## 1. Introduction

The present work is a preliminary investigation to an emission Mössbauer study of the electron-capture after-effects accompanying the radioactive decay of $^{57}$Co into $^{57}$Fe in some $^{57}$Co-doped bivalent oxalates [1]. The dihydrated oxalates, $M^{II}C_2O_4 \cdot 2H_2O$, have been selected due to their well-known crystal structures, allowing characterization of the local environment of the $^{57}$Fe Mössbauer probe with high accuracy. Moreover, a large number of bivalent metals give isomorphous compounds in which the $^{57}$Fe Mössbauer probe can easily be incorporated. Such compounds are therefore particularly convenient to investigate the influence of the host lattice on the chemical after-effects in electron-capture decay of $^{57}$Co into $^{57}$Fe, by incorporating $^{57}$Co in several oxalates of various $M^{2+}$ cations. In order to know exactly the physico-chemical state of the $^{57}$Fe species in the absence of after-effects it is however necessary to register beforehand the absorption spectra of $^{57}$Fe in the same compounds. More information can also be obtained by means of the corresponding mixed crystals of general formula $Fe_{1-x}M_x \cdot C_2O_4 \cdot 2H_2O$.

## 2. Experimental

### *2.1. Syntheses*

$^{57}$Fe-doped dihydrated oxalates, $^{57}$Fe: $M^{II}C_2O_4 \cdot 2H_2O$, with M = Mg, Mn, Fe, Co, Ni and Zn have been synthesized from a solution 0.1 M of the metallic salt (chloride, or sulfate) with 2% at. $^{57}$Fe. Crushed oxalic acid in large excess (50%) is added to the former solution heated at 80 °C; after 10 to 15 min stirring, the precipitate is filtered off and repeatedly washed with boiling water, then dried with alcohol and ether.

Mixed oxalates Fe(II)/Co(II) and Fe(II)/Ni(II) are obtained similarly by co-precipitation from a starting solution containing the respective cations in appropriate proportion.

### *2.2. Structural and Chemical Analysis*

X-ray powder diffraction patterns of preliminary samples obtained under identical working conditions have been registered using a SEIFERT diffractometer with proportional counter and a cobalt-lamp. They indicated in all cases a monoclinic structure corresponding to the α-form of Fe, Co, Ni, Mn and Zn compounds, and to the β-form of the Mg compound.

The water content has been checked by thermogravimetric analysis using a DUPONT 950 analyzer. The respective contents of each cation in mixed crystals have been determined by chemical analysis, namely potentiometric titration of $Fe^{2+}$ with $Ce^{4+}$ in a $H_2SO_4$ 1 M medium, and complexometric titration of $Ni^{2+}$ with EDTA and murexide at pH = 10.

### *2.3. Mössbauer Spectroscopy*

Mössbauer spectra have been registered at room temperature (RT) and 80 K using a constant acceleration transducer coupled with a 512 multichannel analyzer (NORTHERN NS-900), and a $^{57}$Co/Rh source kept at RT. In some particular cases, very accurate measurements of the quadrupole splitting have been obtained using calibration spectra taken just before and after the concerned spectrum. All the isomer shifts (δ) mentioned in the text and the tables are given with respect to metallic α-Fe at RT. Experimental data are resolved into lorentzian lines using an iterative least-squares fit program.

0020-1693/87/$3.50 

## 3. Crystal Structures

The crystal structures of the isomorphous dihydrated oxalates, $M^{II}C_2O_4 \cdot 2H_2O$ have been studied by Deyrieux and Pénéloux for M = Fe [2], M = Mn, Co, Ni and Zn [3]. The monoclinic $\alpha$-form (space group (s.g.) $C2/c$) or the orthorhombic $\beta$-form (s.g. *Cccm*) are observed depending on the particular synthesis conditions.

Only the $\alpha$-form has been observed for Mn and Zn compounds. In the case of Fe, Co and Ni salts, the metastable $\beta$-form precipitates first, changing afterwards into the thermodynamically stable $\alpha$-form, when oxalate ions in excess are available. The latter transformation is promoted by several factors like stirring and heating. A similar study carried out on the $Mg^{2+}$ salt [4] showed the existence of two crystallographic forms both belonging to the monoclinic group (s.g. $C2/c$). The usual synthesis using a $Mg^{2+}$ salt and oxalic acid or alcaline oxalate gives rise to the $\beta$-form which turns into the $\alpha$-form when submitted to prolonged contact with the parent solution.

As pointed out above, the present samples have been identified as monoclinic forms ($\beta$ for Mg, $\alpha$ for all the other compounds); this is due to the particular selected synthesis conditions, *i.e.* precipitation from a hot concentrated solution with oxalic acid in excess.

The metallic atom is octahedrally surrounded by six oxygen atoms, four of them belonging to two coplanar oxalato groups, the two others to two water molecules in *trans* position with respect to the former plane (Fig. 1a, b). The whole structure can be described as a regular packing of parallel sheets, each formed by neighbouring linear $[M(C_2O_4)_2]_n$ chains.

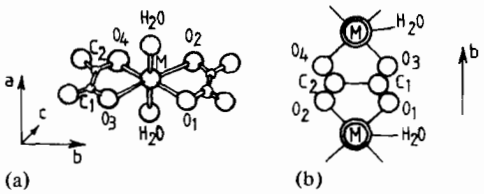


Fig. 1. (a) Octahedral coordination of $M^{2+}$ in dihydrated oxalates, $MC_2O_4 \cdot 2H_2O$. (b) Schematic view of metal–metal bonding projected on (100) plane.

## 4. Results and Discussion

### *4.1. Dihydrated Ferrous Oxalate*

The well-known absorption Mössbauer spectrum of $^{57}Fe$ in $FeC_2O_4 \cdot 2H_2O$ (Fig. 2a) exhibits a quadrupolar doublet whose parameters (at RT: $\Delta = 1.74$ mm $s^{-1}$, $\delta^{Fe} = 1.19$ mm $s^{-1}$) are consistent with high-spin Fe(II) species in a distorted octahedral configuration. Considering the interatomic distances

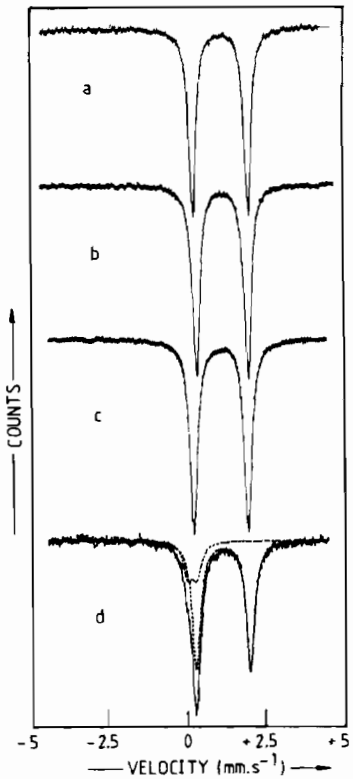


Fig. 2. Absorption Mössbauer spectra of $^{57}Fe$ at 295 K, in (a) $FeC_2O_4 \cdot 2H_2O$, (b) $MnC_2O_4 \cdot 2H_2O$, (c) $NiC_2O_4 \cdot 2H_2O$ and (d) $NiC_2O_4 \cdot 2H_2O$ exposed to air.

given in the literature [2], *i.e.* 211 pm for the Fe–O ($H_2O$) bond and 222 pm for the Fe–O($C_2O_4^{2-}$) bond, the coordination octahedron around the iron atom is found to be compressed along the axis of the two water molecules. Moreover, a previous Mössbauer study [6] of the temperature-dependence of the $^{57}Fe$ quadrupole splitting in $FeC_2O_4 \cdot 2H_2O$ has allowed us to identify the $|xy\rangle$ singlet as the ground state, and to evidence a strong rhombic distortion ($\Delta_1 = 100$ $cm^{-1}$; $\Delta_2 = 960$ $cm^{-1}$). A very accurate measurement of the quadrupole splitting of $^{57}Fe$: $FeC_2O_4 \cdot 2H_2O$ at RT has been performed here, giving $\Delta = 1.742 \pm 0.010$ mm $s^{-1}$; the former value agrees perfectly well with the previously mentioned results listed in Table I (arithmetic mean value: $\Delta = 1.732 \pm 0.026$ mm $s^{-1}$).

### *4.2 $^{57}Fe$ in $M^{II}C_2O_4 \cdot 2H_2O$ (M = Mg, Mn, Co, Ni, Zn)*

The Mössbauer parameters of $^{57}Fe$ in the isomorphous oxalates $M^{II}C_2O_4 \cdot 2H_2O$ have been listed in Table II. Experimental spectra obtained at RT and 80 K are identical with the spectrum of ferrous oxalate (Fig. 2a,b,c), although they present small but significant variations of their quadrupole splitting, which is in any case smaller than in the ferrous

TABLE I. Comparative Mössbauer Parameters of $^{57}$Fe: $FeC_2O_4 \cdot 2H_2O$ from the Literature

| Δ at RT (mm $s^{-1}$) | Reference | |
|---|---|---|
| 1.73 ± 0.01 | Flück | [7] |
| 1.73 | Sano | [8] |
| 1.76 ± 0.03 | Hasley | [9] |
| 1.73 ± 0.03 | Gütlich | [10] |
| 1.74 ± 0.01 | Friedt | [11] |
| 1.71 ± 0.04 | Temperley | [12] |
| 1.71 ± 0.02 | Heidrich | [13] |
| 1.75 | Siekierska | [14] |
| 1.73 ± 0.03 | Caric | [15] |
| 1.70 ± 0.03 | Aramu | [16] |
| 1.742 ± 0.010 | This work | |

compound. The largest differences are observed with Mn and Zn compounds, where Δ goes down to 1.63 and 1.65 mm $s^{-1}$, respectively. Similar effects are observed in the low temperature spectra (Δ = 1.83 and 1.85 mm $s^{-1}$ at 80 K for $MnC_2O_4 \cdot 2H_2O$ and $ZnC_2O_4 \cdot 2H_2O$, respectively, against 2.01 mm $s^{-1}$ for $FeC_2O_4 \cdot 2H_2O$).

As far as we know, only one comparative result has been published in the literature; it concerns $^{57}$Fe in $CoC_2O_4 \cdot 2H_2O$, for which Friedt and Asch [11] have obtained Δ = 1.70 ± 0.03 mm $s^{-1}$ at RT, in total agreement with the present work. They explained this smaller Δ value in the Co compound by invoking the influence on the electric field gradient, of an additional distortion induced by the substitution of $Co^{2+}$ by a bigger $Fe^{2+}$ ion. The present results on the isomorphous oxalates are however inconsistent with such an interpretation, as shown by comparing Δ values with the corresponding ionic radii of the host metals:

$$-r(M^{2+}): Mn > Fe > Co{-}Zn > Mg > Ni$$

$$-\Delta(^{57}Fe{:}M^{2+})\ Fe > Ni > Mg{-}Co > Mn > Zn.$$

Nevertheless, some comments can be made on the dependence of the quadrupole splitting *versus* the 3d-electron configuration of the host metal, as illustrated in Fig. 3 for both measurement temperatures. The main component of the electric field gradient (EFG) tensor, $V_{zz}$, is usually written as

$$V_{zz} = \text{eq} = e[(1 - R)q_{val} + (1 - \gamma_\infty)q_{latt}] \quad (1)$$

where $q_{val}$ and $q_{latt}$ are the respective valence and lattice contributions to the EFG, $e$ is the elementary charge, $R$ and $\gamma_\infty$ are Sternheimer polarization factors.

TABLE II. Mössbauer Parameters of $^{57}$Fe in $M^{II}C_2O_4 \cdot 2H_2O$

| Compound | $T$ (K) | $\Delta^a$ (mm $s^{-1}$) | $\delta^{Fe\ b}$ (mm $s^{-1}$) | $\Gamma^c$ (mm $s^{-1}$) | $I^d$ (%) |
|---|---|---|---|---|---|
| $^{57}Fe{:}FeC_2O_4 \cdot 2H_2O$ | 80 | 2.01 | 1.30 | 0.30 | 100 |
| | 295 | 1.74 | 1.19 | 0.26 | 100 |
| $^{57}Fe{:}CoC_2O_4 \cdot 2H_2O$ | 80 | 1.95 | 1.30 | 0.34 | 100 |
| | 295 | 1.69 | 1.18 | 0.30 | 100 |
| $^{57}Fe{:}NiC_2O_4 \cdot 2H_2O$ | 80 | 1.97 | 1.29 | 0.30 | 100 |
| | 295 | 1.71 | 1.18 | 0.29 | 100 |
| [e] | 80 | 1.96 | 1.30 | 0.40 | 83 |
| | | 0.33 | 0.31 | 0.42 | 17 |
| | 295 | 1.70 | 1.19 | 0.31 | 78 |
| | | 0.28 | 0.21 | 0.34 | 22 |
| $^{57}Fe{:}MnC_2O_4 \cdot 2H_2O$ | 80 | 1.83 | 1.31 | 0.33 | 100 |
| | 295 | 1.63 | 1.20 | 0.28 | 100 |
| $^{57}Fe{:}ZnC_2O_4 \cdot 2H_2O$ | 80 | 1.85 | 1.30 | 0.35 | 100 |
| | 295 | 1.65 | 1.19 | 0.25 | 100 |
| $^{57}Fe{:}MgC_2O_4 \cdot 2H_2O$ | 80 | 1.95 | 1.30 | 0.34 | 100 |
| | 295 | 1.69 | 1.18 | 0.30 | 100 |

[a]Quadrupole splitting (±0.02 mm $s^{-1}$). [b]Isomer shift relative to α-Fe (±0.02 mm $s^{-1}$). [c]Full-width at half maximum (±0.02 mm $s^{-1}$). [d]Relative intensity. [e]Sample exposed to air, partially oxidized.

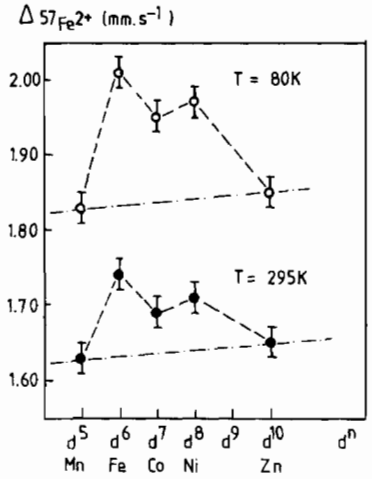


Fig. 3. $^{57}Fe^{2+}$ quadrupole splittings in $^{57}Fe{:}MC_2O_4{\cdot}2H_2O$ *vs.* 3d-electron configuration of the host cation.

For the present purpose, as we compare $^{57}Fe$ states in isomorphous compounds having very similar structural parameters, an effect due to differences in lattice contributions can actually be neglected, firstly, because $q_{latt}$ is generally much smaller than $q_{val}$ in the case of high-spin $Fe^{2+}$, and secondly, because the corresponding variations for different neighbouring $M^{2+}$ ions are very small indeed [2–5]. On the other hand, the valence contribution can be affected by small differences of local electron densities in $Fe^{2+}$ 3d orbitals, resulting from indirect interaction between $Fe^{2+}$ and its neighbouring $M^{2+}$ ions, through the delocalized $\pi$-orbitals of the carboxylate groups of oxalate ligands.

Referring to the separation of $q_{val}$ into two terms originating from crystal field ($q_{CF}$) and molecular orbitals ($q_{MO}$) contributions [17], *i.e.*

$$q_{val} = q_{CF} + q_{MO} \tag{2}$$

where $q_{CF}$ is usually dominant for high-spin $Fe^{2+}$, the neighbouring-effect modifies the minor $q_{MO}$ term. This can be understood by considering the valence contribution to the EFG as a function of imbalance in the 3d-electron populations, as given by

$$q_{val} = \frac{4}{7}\langle r^{-3}\rangle_{3d} \times \left[-n_{3d_{z^2}} + n_{3d_{x^2-y^2}} + n_{3d_{xy}} - \frac{1}{2}(n_{3d_{xz}} + n_{3d_{yz}})\right] \tag{3}$$

where the $n_{3d_i}$ terms represent the respective 3d-orbital populations, which are mainly dependent on temperature and covalency effects.

By separating these two effects, the above expression can also be written as

$$q_{val} = \frac{4}{7}(\langle r^{-3}\rangle_{3d})_0 \ \alpha^2 F(\Delta_1, \Delta_2, T) \tag{4}$$

where the function $F$ expresses the decrease due to Boltzmann population, neglecting spin-orbit coupling, and $\alpha^2 = \langle r^{-3}\rangle/\langle r^{-3}\rangle_0$ is the covalency parameter which expresses the extent of radial expansion of the 3d-orbitals. This parameter usually takes values between 0.6 and 0.9, large $\alpha^2$-values meaning low covalency effects.

Since the $e_g$-orbitals, $3d_{z^2}$ and $3d_{x^2-y^2}$, are involved in localized Fe–O $\sigma$-bonds only, their contributions to $q_{val}$ – which is zero due to single-electron occupancy of each orbital – remains unaltered whatever the host cation be. However, although $C_2O_4^{2-}$ is known as a poor $\pi$-donor ligand, small variations in $\pi$-bonding between $2p_z$ orbitals of the oxygen atom and the $3d_{xz}$, $3d_{yz}$ orbitals of the iron atom can be expected, owing to the delocalization of $\pi$-electrons along the Fe–O–C–O–M chain (Fig. 1b). As the $|xy\rangle$ singlet has been found to be the ground state [6], the $t_{2g}$-orbitals contribution to $q_{val}$, extrapolated at 0 K, can be written as

$$\frac{4}{7}\langle r^{-3}\rangle_{3d}\left[2 - \frac{1}{2}(n_{3d_{xz}} + n_{3d_{yz}})\right] \tag{5}$$

where the $3d_{xz}$ and $3d_{yz}$ populations are affected by the electron configuration of the neighbouring host cation.

According to expression (5), any increase of $d_{xz}$, $d_{yz}$ orbitals population by $\pi$-donor effect will therefore decrease $q_{val}$ and, consequently, the observed quadrupole splitting.

Among the presently investigated cases, significant enhancement of $\pi$-donation will be observed when the electron configuration of 3d-orbitals of the neighbouring metal has a particular stability, *i.e.* with fil- (3) led ($d^{10}$, $Zn^{2+}$), half-filled ($d^5$, $Mn^{2+}$) or empty $d^0$, $Mg^{2+}$) d-orbitals. In the case of $d^7$ ($Co^{2+}$) and $d^8$ ($Ni^{2+}$) configurations, a similar but lower decrease of $\Delta$ is observed, because the 3d electron density is larger than in the iron compound, but without having this particular stability of spherical electronic shells.

The extent of these covalency effects can be estimated from the covalency parameter, $\alpha^2$. If one assumes identical $F$ values for $Fe^{2+}$ in all compounds, because of the same geometry of the iron coordination octahedron [2–5], it is possible to calculate, from $\Delta$ measurements at two temperatures, using expression (4), the covalency parameters relative to the iron compound. These values are listed in Table III, together with absolute estimations of $\alpha_M^2$ using Ingalls value for $FeC_2O_4{\cdot}2H_2O$, *i.e.* $\alpha_{Fe}^2 = 0.80$ [6].

Furthermore, in the case of large $\pi$-donor effect ($Mn^{2+}$), the increasing 3d-electron population reduces the s-electron density at the nucleus by shielding

TABLE III. Relative and Absolute Covalency Parameters of $Fe^{2+}$ in $MC_2O_4 \cdot 2H_2O$

| M | $\alpha_M^2/\alpha_{Fe}^2$ | $\alpha_M^{2\,a}$ |
|---|---|---|
| Mg | 0.96 | 0.77 |
| Mn | 0.74 | 0.59 |
| Fe | 1.00 | 0.80 |
| Co | 0.96 | 0.77 |
| Ni | 0.96 | 0.77 |
| Zn | 0.74 | 0.59 |

[a]Using $\alpha_{Fe}^2 = 0.80$, from ref. 6.

effect; this results in a systematically larger isomer shift in the manganese compound, for which the lowest Δ values are indeed observed.

It appears worth comparing the present results with the observations drawn from previous Mössbauer studies of $^{57}$Fe in other high-spin ferrous compounds.

For example, large variations of the quadrupole splitting have been observed for substitutional $Fe^{2+}$ in some isomorphous carbonates $M^{II}CO_3$, with M = Mg, Ca and Cd [18], M = Co [19] and Zn [20], with respect to siderite, $FeCO_3$ [21]. Similar effects have been evidenced in isomorphous $^{57}$Fe-doped formate dihydrates of several bivalent metals, and will be published later. On the other hand, identical Δ values have been obtained, in mixed crystals of isomorphous sulfate heptahydrates, $Fe_{1-x}M_xSO_4 \cdot 7H_2O$ (M = Mg, Co, Ni, Zn) [22], where $Fe^{2+}$ is coordinated by six water molecules in order to give an octahedron which is insensitive to the influence of the neighbouring metal due to lack of π-electron delocalization.

Nevertheless, from identical isomer shifts and the similarity of Δ values in the series, we are allowed to conclude that the $^{57}Fe^{2+}$ ion enters substitutionally a unique lattice site, which is greatly comparable with the corresponding $Fe^{2+}$ site in the ferrous compound.

It is also interesting to notice that the nickel compound behaves differently from the other oxalates when exposed to air. Whereas ferrous oxalate, as well as all the other $^{57}$Fe-doped oxalates are perfectly stable in ambient air, $Fe^{2+}$ is partially oxidized in the Ni(II) compound when exposed to air for a few days (Fig. 2d). This effect probably results from surface alteration of $^{57}$Fe dopant species, indicating some reluctance to the substitution of the rather small $Ni^{2+}$ ion by a bigger $Fe^{2+}$ ion.

### *4.3 $^{57}$Fe in Mixed Dihydrated Oxalates*

As the Co and Ni compounds presented particular interest for further after-effects studies, a large range of mixed Fe(II)/Co(II) and Fe(II)/Ni(II) oxalates have been investigated in the same way; these measurements allowed us to explain the matrix influence associated with varying Fe concentrations in such compounds.

X-ray powder diagrams are consistent with the obtention of a solid solution on the whole concentration range.

Mössbauer parameters of $^{57}$Fe in these systems are listed in Table IV, where the quadrupole splitting has been measured with high accuracy (±0.010 mm $s^{-1}$). As shown by Figs. 4 and 5 for mixed Fe(II)/Co(II) and Fe(II)/Ni(II) compounds, respectively, a small but significant decrease of the quadrupole splitting is observed for decreasing Fe concentrations. This regular evolution can be considered as additional proof that an homogeneous solid solution has been obtained.

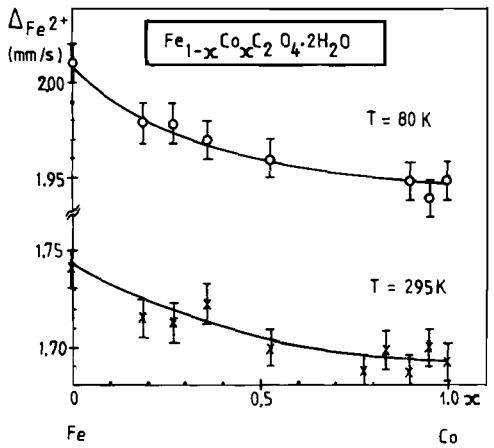


Fig. 4. $^{57}Fe^{2+}$ quadrupole splittings in $Fe_{1-x}Co_xC_2O_4 \cdot 2H_2O$ plotted against Co content in the mixed crystals.

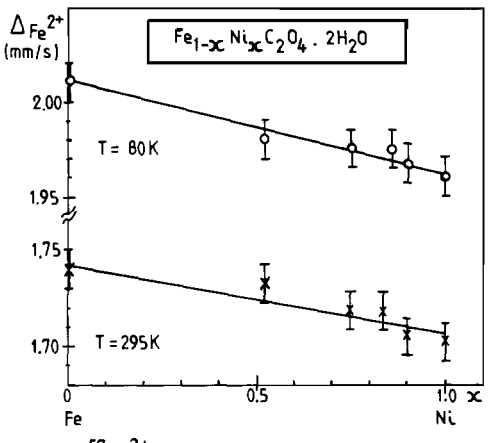


Fig. 5. $^{57}Fe^{2+}$ quadrupole splittings in $Fe_{1-x}Ni_xC_2O_4 \cdot 2H_2O$ plotted against Ni content in the mixed crystals.

Moreover, the decrease of Δ for increasing host metal concentration in the mixed compound is consistent with the indirect electronic influence of the neighbouring cation. As pointed out earlier for the simple compounds, this interpretation is in agree-

TABLE IV. Mössbauer Parameters of $^{57}Fe$ in Mixed Fe(II)/Co(II) and Fe(II)/Ni(II) Dihydrated Oxalates

| Compound | $x$ | $T$ (K) | $\Delta$[a] (mm $s^{-1}$) | $\delta^{Fe}$ (mm $s^{-1}$) | $\Gamma$ (mm $s^{-1}$) |
|---|---|---|---|---|---|
| $FeC_2O_4 \cdot 2H_2O$ | 0.00 | 80 | 2.011 | 1.30 | 0.30 |
| | | 295 | 1.742 | 1.19 | 0.26 |
| $Fe_{1-x}Co_xC_2O_4 \cdot 2H_2O$ | 0.19 | 80 | 1.979 | 1.31 | 0.29 |
| | | 295 | 1.716 | 1.19 | 0.30 |
| | 0.27 | 80 | 1.979 | 1.31 | 0.34 |
| | | 295 | 1.713 | 1.19 | 0.28 |
| | 0.36 | 80 | 1.970 | 1.32 | 0.36 |
| | | 295 | 1.724 | 1.20 | 0.30 |
| | 0.53 | 80 | 1.960 | 1.31 | 0.31 |
| | | 295 | 1.699 | 1.19 | 0.26 |
| | 0.78 | 295 | 1.686 | 1.19 | 0.26 |
| | 0.84 | 295 | 1.699 | 1.19 | 0.35 |
| | 0.90 | 80 | 1.948 | 1.30 | 0.36 |
| | | 295 | 1.686 | 1.19 | 0.25 |
| | 0.95 | 80 | 1.938 | 1.31 | 0.33 |
| | | 295 | 1.700 | 1.20 | 0.25 |
| | 1.00 | 80 | 1.949 | 1.30 | 0.34 |
| | | 295 | 1.692 | 1.18 | 0.30 |
| $Fe_{1-x}Ni_xC_2O_4 \cdot 2H_2O$ | 0.52 | 80 | 1.981 | 1.31 | 0.43 |
| | | 295 | 1.734 | 1.20 | 0.34 |
| | 0.75 | 80 | 1.976 | 1.30 | 0.41 |
| | | 295 | 1.719 | 1.19 | 0.41 |
| | 0.86 | 80 | 1.976 | 1.29 | 0.35 |
| | | 295 | 1.719 | 1.18 | 0.40 |
| | 0.90 | 80 | 1.968 | 1.29 | 0.41 |
| | | 295 | 1.706 | 1.18 | 0.29 |
| | 1.00 | 80 | 1.962 | 1.29 | 0.30 |
| | | 295 | 1.704 | 1.18 | 0.29 |

[a] $\pm 0.010$ mm $s^{-1}$.

ment with the absence of $\Delta$ variations in mixed crystals of sulfate heptahydrates [22].

The present measurements concerning the Fe/Ni system do not agree with previous results published by Ramani *et al.* [23]; through lack of accurate measurements, these authors failed to detect any significant variation of $\Delta$ in the series, but they reported a quite large increase of the isomer shift (+0.12 mm $s^{-1}$) for $x > 0.75$, which cannot easily be explained. Namely, this behaviour seems in total disagreement with an eventual pressure effect due to the more compact structure of the nickel compound; this would result in decreasing $\delta$ and increasing $\Delta$ values, if experimentally detectable. Such experiments performed by Champion *et al.* [24] on $FeC_2O_4 \cdot 2H_2O$ indicated that an external pressure of 25 kbar caused only very small $\delta$ variations (−0.04 mm $s^{-1}$) but a significant $\Delta$ increase (+0.27 mm $s^{-1}$).

## Acknowledgements

The authors greatly acknowledge the Institut Interuniversitaire des Sciences Nucléaires, Brussels, for financial assistance, and Ph. Hennaux for his help in chemical analysis.

## References

1 M. Devillers, J. Ladrière and D. Apers, to be published.
2 R. Deyrieux and A Pénéloux, *Bull. Soc. Chim. Fr., 8,* 2675 (1969).
3 R. Deyrieux, C. Berro and A. Pénéloux, *Bull. Soc. Chim. Fr., 1,* 25 (1973).
4 L. Walter Levy and J. Perrotey, *Bull. Soc. Chim. Fr., 5,* 1697 (1970).
5 L. Walter Levy, J. Perrotey and J. W. Visser, *Bull. Soc. Chim. Fr., 3,* 757 (1971).
6 R. Ingalls, *Phys. Rev., 133,* 3A, 787 (1964).
7 E. Fluck, W. Kerler and W. Neuwirth, *Angew. Chem. Int. Edit. Engl., 2,* 277 (1963).
8 H. Sano and F. Hashimoto, *Bull. Chem. Soc. Jpn., 38,* 1565 (1965).
9 M. J. Hasley and A. M. Pritchard, *J. Chem. Soc. A,* 2878 (1968).
10 P. Gutlich, S. Odar, B. W. Fitzsimmons and N. E. Erickson, *Radiochim. Acta, 10,* 147 (1968).

11 J. M. Friedt and L. Asch, *Radiochim. Acta, 12,* 208 (1969).
12 A. A. Temperley and D. W. Pumplin, *J. Inorg. Nucl. Chem., 31,* 2711 (1969).
13 W. Heidrich, *Z. Phys., 230,* 418 (1970).
14 K. E. Siekierska and J. Fenger, *Radiochim. Acta, 14,* 93 (1970).
15 S. Caric, L. Marinkov and J. Slivka, *Phys. Stat. Sol., (a) 13,* 263 (1975).
16 F. Aramu, V. Maxia and C. Muntoni, *Lett. Nuovo Cim., 12,* 225 (1975).
17 G. M. Bancroft, 'Mössbauer Spectroscopy', Mc Graw-Hill, London, 1973, p. 29.
18 K. K. P. Srivastava, *J. Phys. C: Solid St. Phys., 16,* L1137 (1983).
19 H. Nam Ok, *Phys. Rev., 181,* 563 (1969).
20 D. C. Price, C. E. Johnson and I. Maartense, *J. Phys. C: Solid St. Phys., 10,* 4843 (1977).
21 D. L. Nagy, I. Deszi and U. Gonser, *Neues Jahrb. Mineral., Monatsh., 3,* 101 (1975).
22 W. Siebke, H. Spiering and E. Meissner, *Phys. Rev. B, 27,* 2730 (1983).
23 Ramani, M. P. Sathyavathiamma, N. G. Puttaswamy and R. M. Mallya, *Phys. Stat. Sol., (a) 77,* 87 (1983).
24 A. R. Champion, R. W. Vaughan and H. G. Drickamer, *J. Chem. Phys., 47,* 2583 (1967).